AIAA JOURNAL
Vol. 31, No. 1, January 1993

Strong Vibrational Nonequilibrium in Supersonic Nozzle Flows

A. Chiroux de Gavelle de Roany,* C. Flament,† J. W. Rich,‡ and V. V. Subramaniam§
Ohio State University, Columbus, Ohio 43210
and
Walter R. Warren Jr.¶
Pacific Applied Research, Rancho Palos Verdes, California 90274

A model and numerical code are presented that describe quasi-one-dimensional compressible flows of gases with nonequilibrium of their vibrational and electronic energy modes. Chemical reaction channels are also modeled. Rate equations governing individual vibrational state populations are integrated as a function of streamwise position in a flow channel. Results are presented for flows of CO, N_2, and NO in supersonic nozzles, and the conditions creating extreme nonequilibrium overpopulation of upper vibrational states are shown. Applications to ^{13}C isotope separation processes, to possible vibration-to-electronic and electronic-to-electronic mode energy transfer lasers, are discussed.

Introduction

CHEMICALLY reactive flows of compressible gases are extensively studied, with interest renewed by current hypersonic flight problems,[1-3] nonequilibrium molecular electric discharge reactors,[4] and investigations of new gas lasers.[5] In each of these applications, it is recognized that, in addition to chemical nonequilibrium, nonequilibrium of the molecular vibrational modes can often be a major influence. This is particularly the case in thermodynamic environments in which the translational and rotational molecular energy modes are maintained in equilibrium at a relatively low temperature, while the vibrational molecular mode(s) have high specific energies. Such environments are commonly realized in supersonic expansions of gases at high stagnation enthalpies, in molecular electric glow discharge plasmas, and in optically pumped molecular gases. In these cases, inelastic collisions exchanging vibrational energy can create extreme non-Boltzmann populations of vibrational energy states; these are so-called vibration-vibration (V-V) pumped environments.[6,7] Historically, vibrationally nonequilibrium flow environments have been the subject of detailed modeling for certain gas and gas-dynamic laser species.[8-10] Such studies have, however, been largely confined to investigations of relatively low-lying vibrational states and, in the case of chemical laser flows, to chemical processes directly relevant to pumping a vibrational population inversion.

The present study addresses the processes influencing the populations of very high vibrational quantum states of diatomic gas molecules in nonequilibrium gas dynamic flows. Specifically, while it is well known that vibration-vibration pumping processes can populate high vibrational levels, the mechanisms that limit such up-pumping, which include chemical reaction and vibration-to-electronic (V-E) mode energy transfer, are only beginning to be understood.[11-14] We report here detailed modeling studies of supersonic expansion flows of CO and N_2, with energy transfer into low-lying excited electronic states. We discuss the nozzle conditions that create extreme upper vibrational state disequilibrium. A critical survey of recent theoretical and experimental vibration-state-specific energy transfer data for these species has been conducted and relevant rate data have been incorporated into the kinetic model. Three major applications of the model are discussed:

1) Isotopic separation of ^{13}C by V-V pumping; related separation processes can occur in other molecules.

2) Possible V-E energy transfer lasers, such as CO to NO, or N_2 to NO, and other systems.

3) Possible electronic-to-electronic (E-E) energy transfer lasers.

A computer modeling code has been developed and applied to these problems. The code includes kinetic equations for vibrational level populations of up to five diatomic molecular species, including excited electronic states of some of these species. The kinetic equations are fully coupled to the gas dynamic conservation equations.

The details of the model are outlined, including the governing equations, the specific kinetic rate models, and the method of computer integration used. We discuss gas dynamic nozzle design to maximize populations on very high vibrational levels. Then, we present computed results and give a brief summary and review of model extensions currently in progress. The Appendix gives the detailed analytic rate expressions used.

Model

Assumptions

The rapid expansion through a two-dimensional planar nozzle is modeled with a quasi-one-dimensional approach. The flow is assumed to be inviscid and compressible, and we are only interested in the steady-state solution. The translational and rotational energy modes are supposed to be in full equilibrium along the nozzle, so that a single temperature can be defined for these modes. This approximation neglects the extremely short relaxation times for rotational and translational equilibration (processes typically requiring a few molecular collisions).

The vibrational energy modes can follow a non-Boltzmann distribution and take into account the anharmonicity of the molecules. The diatomic molecules are electronically active and each electronic state is counted as a separate species. The monatomic species are treated as simple diluents that participate only in vibration-translation processes and chemistry.

Presented as Paper 90-0252 at the AIAA 26th Aerospace Sciences Meeting, Reno, NV, Jan. 8-11, 1990; received Dec. 2, 1991; revision received March 30, 1992; accepted for publication April 21, 1992.

*Graduate Research Associate; currently at Automobile Peugeot, Av. Jean-Pierre Timbaud, Poissy 78000, France.

†Postdoctoral Fellow, Department of Mechanical Engineering, 206 W. 18th Avenue.

‡Professor, Department of Mechanical Engineering, 206 W. 18th Avenue. Member AIAA.

§Assistant Professor, Department of Mechanical Engineering, 206 W. 18th Avenue. Member AIAA.

¶President, 6 Crestwind Drive. Fellow AIAA.

Balance Equations

The mass conservation equation for quasi-one-dimensional flows is

$$\rho u A = \text{const} \tag{1}$$

where u is the streamwise gas velocity component along the nozzle, ρ the density of the gas, and $A = A(x)$ the cross-sectional area of the nozzle. The conservation equation governing the population of the vth vibrational state of the diatomic species i is

$$\frac{\rho u}{m_i}\frac{\mathrm{d}Y_{i,v}}{\mathrm{d}x} = \mathrm{VV}_i^v + \mathrm{VT}_i^v + \mathrm{VE}_i^v + \mathrm{EE}_i^v + \mathrm{SRD}_i^v + \mathrm{CHM}_i^v \tag{2a}$$

where m_i is the molecular mass of species i, $Y_{i,v} = \rho_{i,v}/\rho$ is the mass fraction of the vibrational state v of the species i, and $\rho_{i,v}$ is the density of the species i in the vibrational state v.

The right-hand side of Eq. (2a) is the sum of various inelastic collision processes that change the vibration state or the chemical species. VV represents the sum of the rate processes changing vibrational state by molecular collisions which exchange vibrational mode energy (vibration-vibration exchange). VT and VE represent changes of vibrational state by exchange of energy between vibrational modes and translational/rotational modes, and between vibrational and electronic modes, respectively. EE represents the exchange of energy between two electronically excited molecules by nonradiative collisional processes. SRD represents the change of vibrational state by spontaneous radiative decay processes. Finally, CHM represents changes of state and species by chemical reactions. The details of these expressions are given in the Appendix.

The conservation equation governing the population of a monatomic species m is:

$$\frac{\rho u}{m_m}\frac{\mathrm{d}Y_m}{\mathrm{d}x} = \mathrm{CHM}_m \tag{2b}$$

The momentum and energy equations, where p is the pressure and h the enthalpy per unit mass of the mixture, are given, respectively, by

$$\frac{\mathrm{d}p}{\mathrm{d}x} + \rho u\frac{\mathrm{d}u}{\mathrm{d}x} = 0 \tag{3}$$

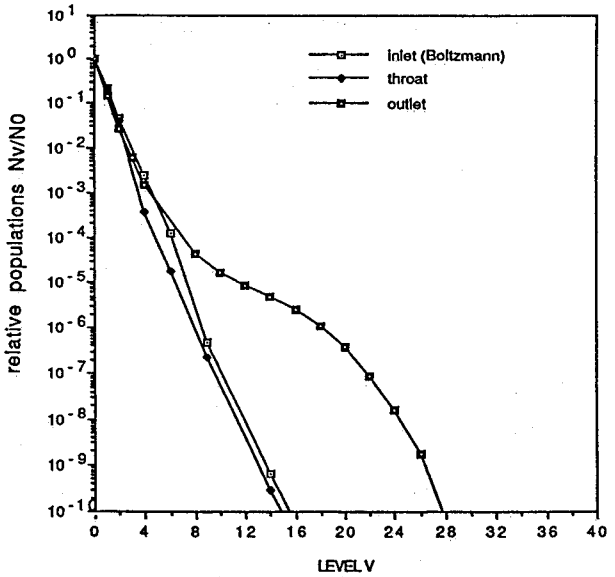

Fig. 1 Normalized vibrational populations vs vibrational quantum number: pure CO; P_0 = 100 atm; T_0 = 2000 K; outlet: P = 17.5 Torr; T = 199 K; M = 7.1; A/A^* = 110.

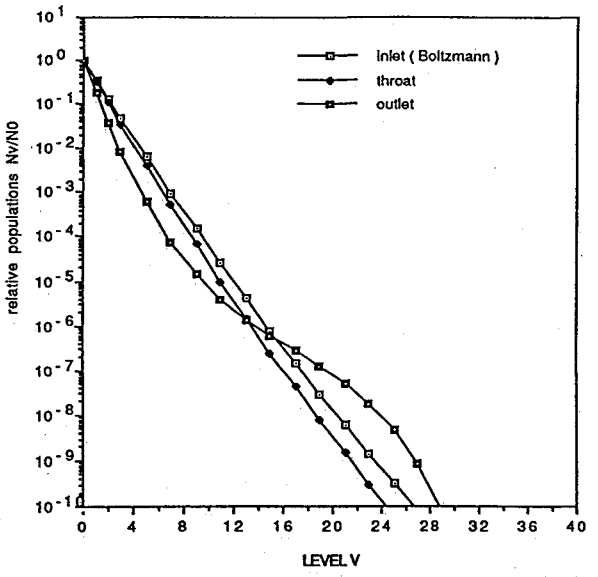

Fig. 2 Normalized vibrational populations vs vibrational quantum number: pure CO; P_0 = 100 atm; T_0 = 2000 K; outlet: P = 17.5 Torr; T = 327 K; M = 6.9; A/A^* = 110.

$$\frac{\mathrm{d}}{\mathrm{d}x}[h + \tfrac{1}{2}u^2] = -q_r \tag{4}$$

where q_r is the energy sink due to radiative transitions, which are expected to be optically thin.

Thermodynamic Equations

The average mass and pressure of the mixture are, respectively,

$$\frac{1}{\mu} = \sum_{i,v}\frac{Y_{i,v}}{m_i} + \sum_m \frac{Y_m}{m_m} \tag{5}$$

$$p = \frac{\rho}{\mu}kT \tag{6}$$

where k is the Boltzmann constant.

The average enthalpy per unit mass of the mixture is

$$h = \frac{5}{2}\frac{kT}{\mu} + \sum_{i,v}\frac{Y_{i,v}}{m_i}(kT + E_{i,v} + h_i^o) + \sum_m Y_m(Te_m + h_m^o) \tag{7}$$

where $E_{i,v}$ is the internal energy of molecule i in vibrational level v for a given electronic state, Te_i the electronic energy, and h_i^o the heat of formation per unit mass of species i. $E_{i,v}$ is given by

$$E_{i,v} = Te_i + \omega_{ei}(v + \tfrac{1}{2}) - \omega_{ei}x_{ei}(v + \tfrac{1}{2})^2 \tag{8}$$

where ω_{ei} and x_{ei} are the spectroscopic constants (fundamental vibrational frequency and anharmonicity, respectively) for the molecule i.

System of Ordinary Differential Equations Solved

Additional assumptions include constant average mass μ (which is justifiable for the reactions under consideration here). There is only one monatomic species m, the radiation energy sink is negligible, and the effect of the enthalpy of formation on the mixture total energy is negligible (the products are assumed to be in very small quantity).

With these assumptions, the previous equations can be written in terms of the derivatives of the molar fractions $X_{i,v} = Y_{i,v}\mu/m_i$ of the velocity u, and of the translational/rotational temperature T:

$$\rho u A = \text{const} \tag{9a}$$

$$X_m = 1 - \sum_{i,v} X_{i,v} \tag{9b}$$

$$\frac{dX_{i,v}}{dx} = \frac{\mu}{\rho u}(VV_i^v + VT_i^v + VE_i^v + EE_i^v + SRD_i^v + CHM_i^v) \tag{9c}$$

$$\frac{du}{dx} = -\frac{u}{(1-M^2)}\left\{\frac{dA}{A\,dx} + \Phi\right\} \tag{9d}$$

$$\frac{dT}{dx} = T\left\{\frac{1}{A}\frac{dA}{dx} + \left(1 - \frac{\mu u^2}{kT}\right)\frac{1}{u}\frac{du}{dx}\right\} \tag{9e}$$

where M is the Mach number based on the frozen speed of sound and Φ is a function that couples the equations of gas dynamics to the kinetics:

$$M = u/a \tag{10a}$$

$$a^2 = \frac{kT}{\mu}\left\{\frac{(5/2) + \sum_{i,v} X_{i,v}}{(3/2) + \sum_{i,v} X_{i,v}}\right\} \tag{10b}$$

$$\Phi = \frac{1}{(5/2) + \sum_{i,v} X_{i,v}}\left[\sum_{i,v}\left(\frac{E_{i,v}}{kT} + 1\right)\frac{dX_{i,v}}{dx}\right] \tag{10c}$$

Numerical Approach and Applications

The nozzle consists of two profiles for the subsonic and supersonic expansions. The zone from the entrance to the throat has a parabolic shape. Immediately downstream of the throat, the supersonic expansion is straight walled, with a specified expansion half-angle. The throat height is taken to be 0.0048 m, with the entrance height being 0.48 m. The channel width is taken to be 0.01 m. The influence of an additional constant area channel, downstream of the expansion, is also studied; the location of this channel extension is varied parametrically. In our calculations, the stagnation conditions are chosen to be those generated by a shock tunnel, typically: $T_0 = 2000$ K and $P_0 = 100$ atm. The gas is chemically, vibrationally, and electronically active. The set of the fully coupled equations is solved using a stiff equation integrator LSODE.[5,16]

For the cases studied, which include several vibrationally active species, this system represents between 100 and 200 stiff equations. They have been integrated from the subsonic section through to the supersonic-hypersonic expansion. The integration through the throat represents a singularity; in some

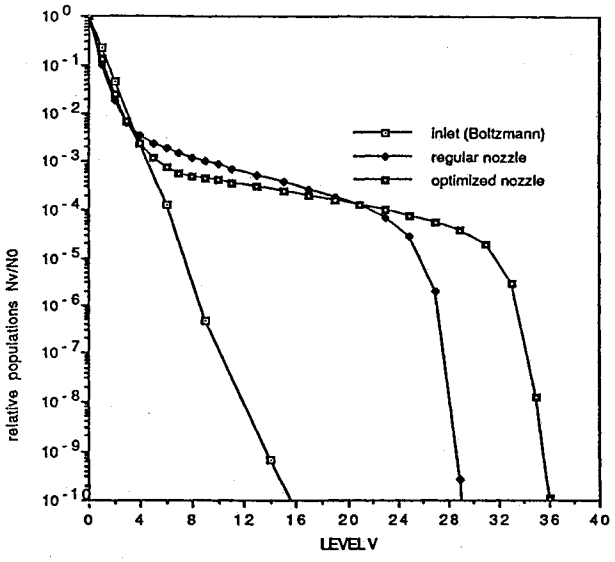

Fig. 3 Normalized vibrational populations vs vibrational quantum number: 20% CO-80% Ar; $P_0 = 100$ atm; $T_0 = 2000$ K; regular nozzle outlet: $P = 5.7$ Torr; $T = 59$ K; $M = 11.5$; $A/A^* = 111$; optimized nozzle outlet: $P = 31.4$ Torr; $T = 116$ K; $M = 7.8$; $A/A^* = 41$.

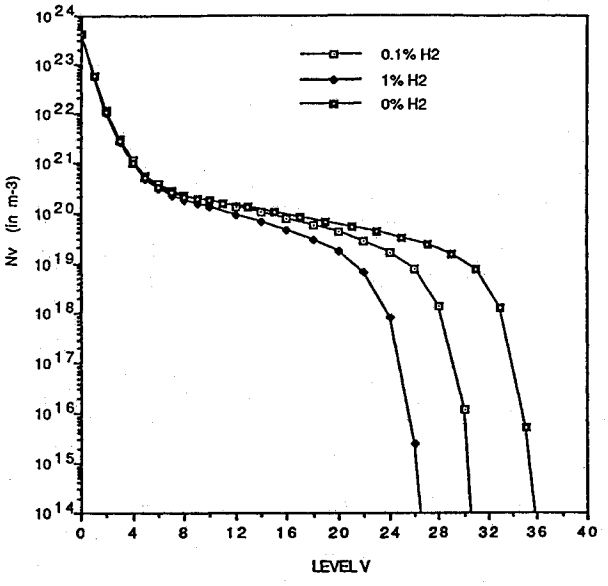

Fig. 4 Vibrational populations vs vibrational quantum number: H_2 impurity influence; CO-Ar-H_2, optimized nozzle.

previous calculations, this has been avoided by assuming that the gas is in Boltzmann equilibrium at the throat. Our calculations show that the flow through the subsonic channel creates an out-of-equilibrium vibrational distribution of the molecules at the throat. The vibrational distribution of CO is plotted for a 15-deg half-angle expansion nozzle at two locations: at the nozzle inlet where CO is at equilibrium, and at the throat (Figs. 1 and 2). Other run parameters are specified in the figure.

Since there is clearly a small, but not necessarily negligible nonequilibrium effect at the throat, we have chosen to integrate the system from the subsonic section to the supersonic expansion. An initial Mach number is calculated at the inlet of the nozzle; it is determined by considering the isentropic expansion of a nonactive gas ($\gamma = 1.4$). This inlet Mach number is changed each time the Mach number decreases during the expansion. An iterative scheme is then set up, using a halving method for calculating the new inlet Mach number.

Design for High Vibration-to-Vibration Up-Pumping

Effect of the Mixture

When expanding pure CO through a 15-deg half-angle nozzle, the vibrational distribution of CO begins to show strong non-Boltzmann populations downstream of the throat. For example, as shown in Fig. 1, there is a considerable up-pumping of populations for levels lying between $v = 8$ and 26 at the nozzle outlet. As shown in Figs. 1 and 2, V-T relaxation is active downstream in the nozzle and is increased if the stagnation temperature is raised from 2000 to 3000 K. Argon is added to CO in order to decrease the V-T relaxation; this is possible because the V-T rate for Ar-CO is less than the V-T rate for CO-CO. Ar acts as a coolant in the mixture and allows CO to be more strongly pumped on its vibrational levels below $v = 25$, as shown in Fig. 3. It may be noted that partial vibrational population inversions of the type shown, produced in supersonic expansions of CO-Ar mixtures, constitute the typical gas dynamic CO laser environment,[17] which was first studied both theoretically and experimentally by McKenzie.[9]

To study the effect of the V-T relaxation and to assess the effect of possible impurities present in the mixture, we have calculated the CO vibrational distribution when the mixture consists of CO, Ar, and H_2. Figure 4 shows the vibrational distribution of CO expanding in an optimized nozzle for several percentages of H_2 in the mixture. The CO-H_2 V-T relaxation is very fast, and as the percentage of H_2 increases, CO is less excited on its high vibrational levels. It appears that, for

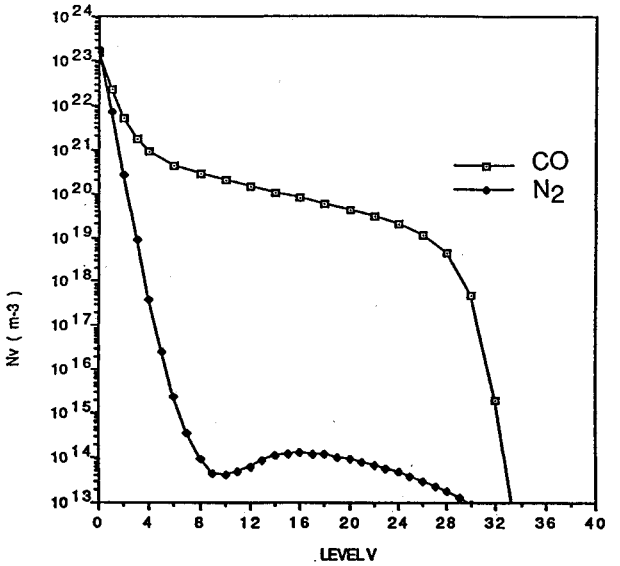

Fig. 5 Vibrational populations vs vibrational quantum number: 20% CO-20% N_2-60% Ar; regular nozzle; outlet: $P = 8.7$ Torr; $T = 90.9$ K; $M = 9.1$; $A/A^* = 111$.

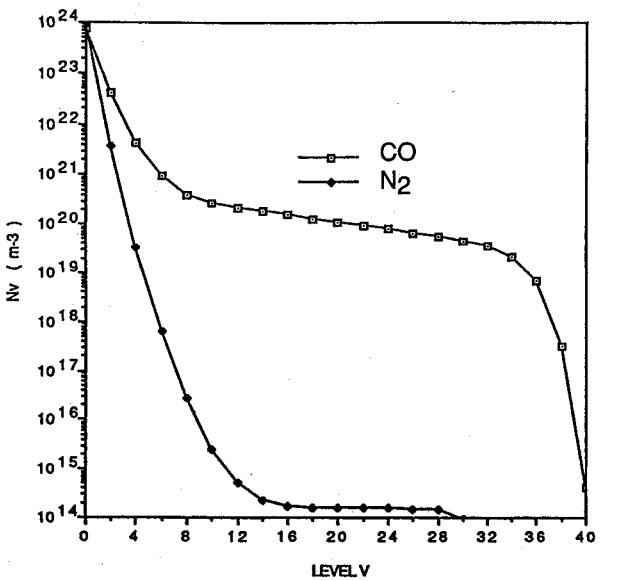

Fig. 6 Vibrational populations vs vibrational quantum number: 20% CO-210% N_2-60% Ar; optimized nozzle; $P = 103$ Torr; $T = 209$ K; $M = 5.8$; $A/A^* = 22$.

less than 1% H_2, CO remains highly excited. We are presently reviewing CO-H rate constants in order to investigate the relaxation of CO by atomic hydrogen during the expansion; H relaxes CO even more efficiently than H_2 does. Such studies are necessary since possible water vapor or hydrocarbon impurities can partially dissociate under some nozzle plenum conditions, providing H_2 and H, which weaken the influence of V-V up-pumping.

Dramatic nonequilibrium vibrational energy partition has been observed when expanding a mixture CO-N_2-Ar. The average energy per particle is plotted in Fig. 7a for CO and N_2 expanding along the nozzle. The energy is significantly transferred from N_2 to CO during the supersonic expansion, which enhances the excitation of the high energy levels in CO (Figs. 5 and 6). This energy partition is a consequence of the well-known preferential transfer of vibrational energy from the more widely spaced vibrational quantum levels to the more closely spaced vibrational quantum levels in V-V pumped systems.[6] In this example, the higher the frequency, more widely spaced N_2 levels transfer energy to the CO. It should be noted

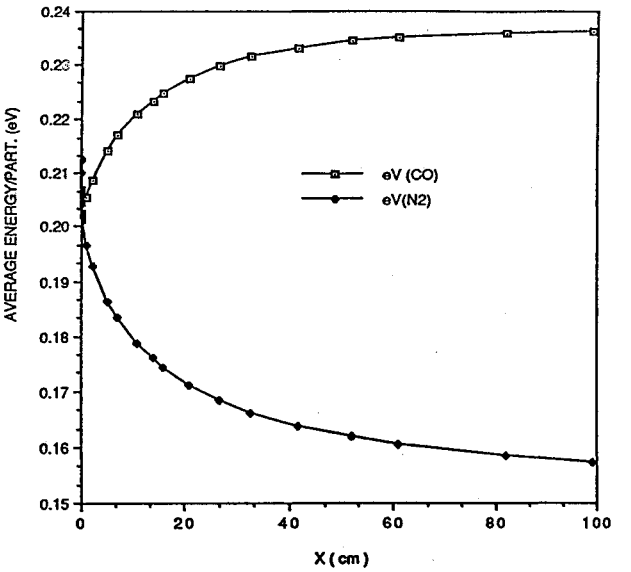

Fig. 7a Average vibrational mode energy vs nozzle position: mixture CO-N_2-Ar.

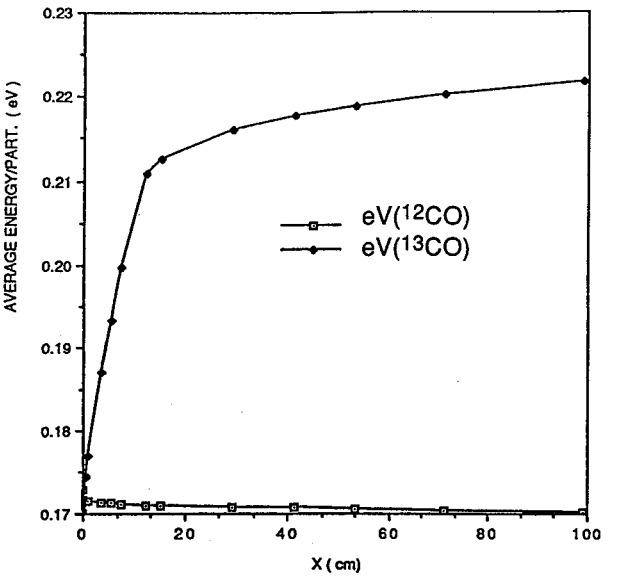

Fig. 7b Average vibrational mode energy vs nozzle position: mixture ^{12}CO-^{13}CO-Ar.

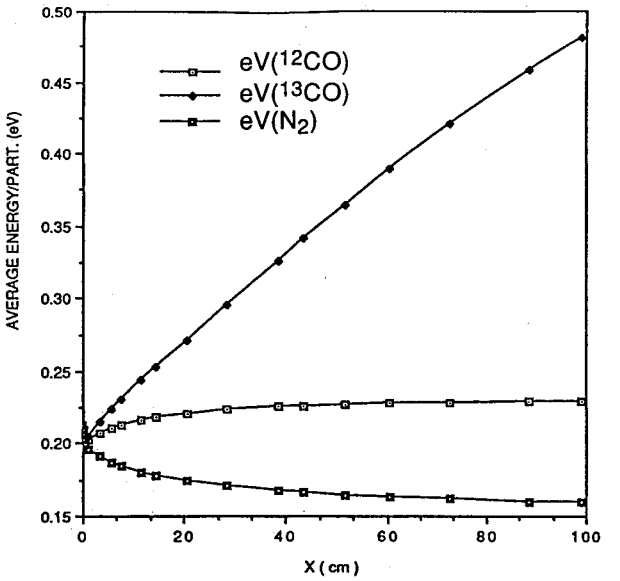

Fig. 7c Average vibrational mode energy vs nozzle position: mixture ^{12}CO-^{13}CO-N_2-Ar.

that the N_2 distribution of Fig. 5, which now contains relatively low energy, displays the total population inversion over some states, which characterizes so-called weak pumping cases. In most subsequent calculations we use mixtures of CO-N_2-Ar to provide highly pumped CO vibrational distributions.

Effect of the Nozzle Geometry

In most numerical simulations, with a mixture providing pumped distributions of CO, the first few vibrational levels have a high density compared to levels of about $v = 25$–30. To drain vibrational quanta from the low levels up to the high-lying levels, one has to flow the mixture through a constant area channel, thus stopping the expansion in the supersonic section. The combination of the nozzle and the additional straight channel is referred to here as the optimized nozzle. The location of the straight channel is found by considering the energy transfer curves (Figs. 7a–c). For the mixture CO-N_2-Ar, which was just considered, the energy transfer curve (Fig. 7a) shows a saturation in the transfer 20 cm after the throat; we choose this location for stopping the supersonic expansion with a straight channel. Figures 5 and 6 show the vibrational distribution of CO expanding in a nozzle without a straight channel (regular nozzle) and in an optimized nozzle, respectively. The improvement is obvious; with the optimized nozzle, although the low levels are less populated, the distribution is pumped up to level $v = 38$ instead of 30 with the regular nozzle. The effect of the straight channel is also demonstrated in Fig. 3 with a CO-Ar mixture.

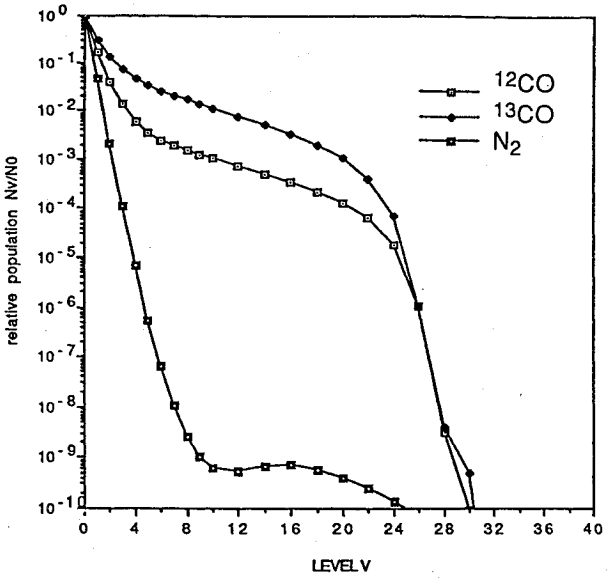

Fig. 8 Normalized vibrational populations vs vibrational quantum number: 25% CO-25% N_2-50% Ar; outlet: $P = 8.2$ Torr; $T = 109$ K; $M = 8.4$; $A/A^* = 111$.

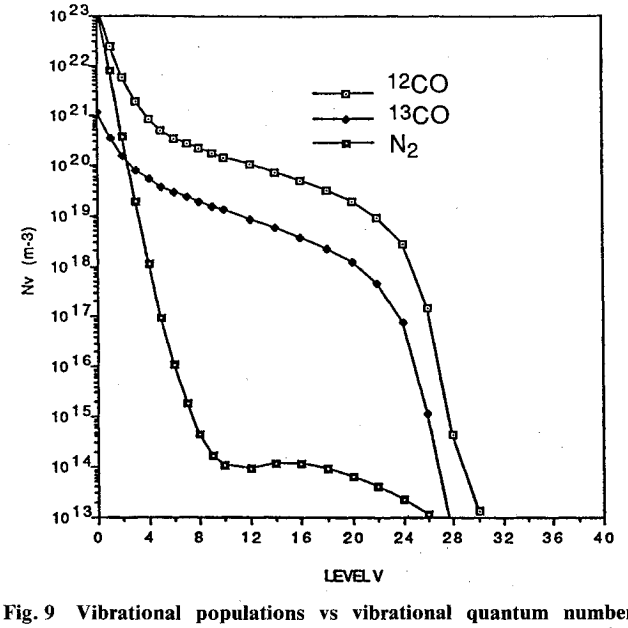

Fig. 9 Vibrational populations vs vibrational quantum number: 25% CO-25% N_2-50% Ar; outlet: $P = 8.2$ Torr; $T = 109$ K; $M = 8.4$; $A/A^* = 111$.

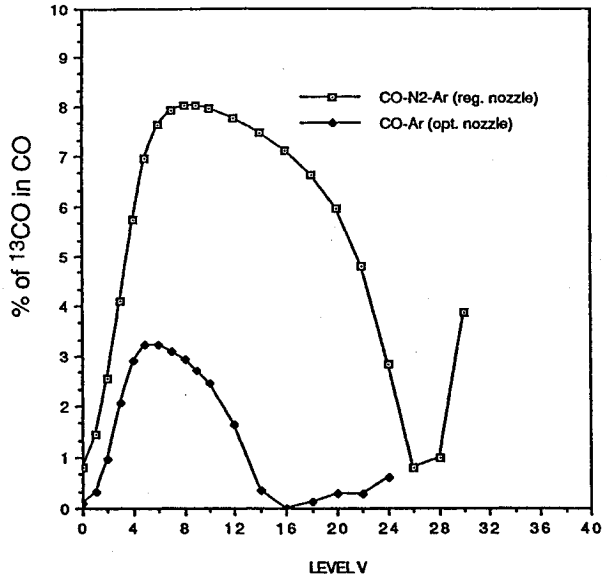

Fig. 10 ^{13}C isotopic enrichment vs vibrational quantum number: natural abundance: 1.1%.

Clearly, the present inviscid, shock-free calculations represent an optimum that can only be approached experimentally by a carefully contoured nozzle design with due allowance for boundary-layer displacement. We note, however, that CO gas laser experiments in a relatively low density, planar 15-deg half-angle nozzle produce a supersonic near-isentropic core that approximates the velocity/temperature distribution given by the model.[18]

Results

The following diatomic molecules are investigated. Unless indicated otherwise, molecules are in their electronic ground state: $^{12}C^{16}O$, $^{13}C^{16}O$, CO($a^3\Pi$), N_2, NO($X^2\Pi$), NO($B^2\Pi$). Simplified energy level diagrams for the CO and NO species are given in Fig. 12. Ar is added in most mixtures. C and CO_2 appear as reaction products; they can relax active molecules by V-T transfer.

Both isotope separation and energy transfer laser applications involving excited electronic states (V-E, E-E, chemical reactions) require that relatively high vibrational levels of CO be populated. In most cases, we require a density of about $10^{-5}N_0$ for vibrational levels of CO from $v = 20$ to 35, N_0 being the number density of the vibrational ground state $v = 0$. Our optimized nozzle expansion will cause energy transfer processes to give such high populations on the upper vibrational levels.

Isotope Separation

The basic mechanism of the separation of ^{13}C is the following: a vibrational energy transfer occurs from ^{12}CO to ^{13}CO; Figs. 7b and 7c show the evolution of the average energy per particle along the nozzle for the two isotopes. The energy is clearly transferred from ^{12}CO to ^{13}CO. This is again an example of preferential transfer of vibrational energy favoring the lower frequency, more closely spaced quantum levels of the ^{13}CO.[6,7] The vibrational distributions of the two isotopes are plotted in Figs. 8 and 9 for the case when N_2 and Ar are added

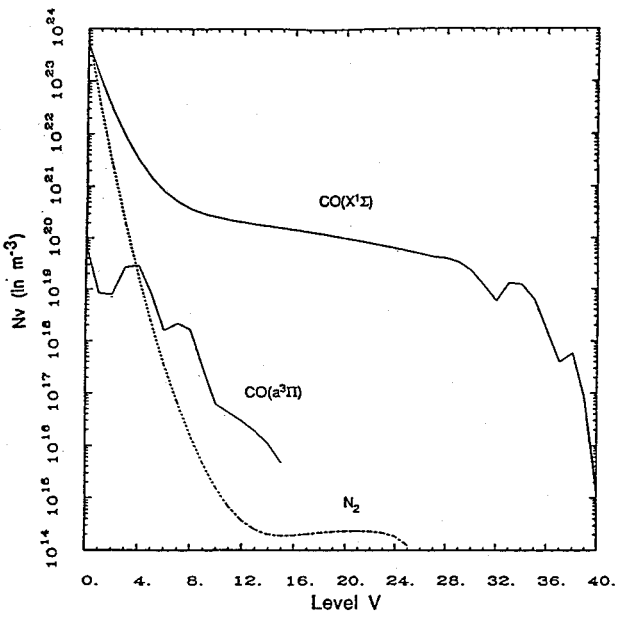

Fig. 11 Vibrational populations vs vibrational quantum number: influence of excited electronic states: 10% CO-10% N_2-80% Ar: $S^0_{VE} = 5 \times 10^{-13}$ cm^3/s; $S^0_{VE}/k_0 = 100$.

to the mixture. The vibrational distribution of ^{13}CO is pumped more efficiently than the ^{12}CO distribution. The natural abundance of ^{13}CO is 1.1%; the percentage of ^{13}CO in CO vs the vibrational state is plotted in Fig. 10. There is a preferential excitation in ^{13}CO for some states occurring in the mixture; the maximum is at $v = 10$, ^{13}CO representing about 8% of CO in the state $v = 10$. The best case is obtained by using an optimized nozzle; the straight channel is located 20 cm after the throat.

An enrichment product can be obtained by considering the following reactions, which take place all along the expansion:

$$CO(X^1\Sigma^+, v) + CO \rightarrow CO_2 + C$$

$$CO(a^3\Pi, w) + CO \rightarrow CO_2 + C$$

The reactants are either ^{12}CO or ^{13}CO, and the products are ^{12}C, ^{13}C, $^{12}CO_2$, or $^{13}CO_2$. From earlier experiments,[19] the channel forming $^{13}CO_2$ seems to be the most probable. We are presently introducing these chemical reactions and energy transfer into the first excited electronic state, $CO(a^3\Pi)$, in the code (see the following subsections). The model can be compared with experiments in which the CO_2 that was produced during the expansion is removed with a liquid nitrogen trap, and the actual enrichment in $^{13}CO_2$ is analyzed.[20,21]

The effective activation energy of the preceding reactions is about 6 eV, which represents a vibrational level of about $v = 25$ for $CO(X^1\Sigma)$, or a low-lying vibrational level of $CO(a^3\Pi)$. Thus, it is necessary to transfer as much energy as possible to ^{13}CO in order to provide the required activation energy. It seems that if we can provide a fair density of $^{13}CO(v > 20)$, a high enrichment can be reached. The limit $v > 20$ is somewhat uncertain since the rate constants of the chemical reaction and of the electronic transfer from $CO(X^1\Sigma)$ to $CO(a^3\Pi)$ are not well known. Further experiments that are presently underway should enable assessment of an efficient separation of ^{13}C when compared with the results of this study.

Monitoring the amount of C and CO_2 produced, we have observed that only a small amount of these products are formed during the expansion. If we calculate the ratio of the density of CO_2 produced to the total density of CO, we find CO_2/CO between 10^{-3} and 10^{-6}, depending on the conditions we have considered. The yield of the chemical reactions is therefore very low; since the pressure of CO does not generally exceed 200 Torr at the end of the expansion, it is unlikely that such a process could be practically used for isotope separation, unless one can use a very long straight channel and operate the supersonic expansion for several seconds. Nevertheless, short duration supersonic expansion experiments have been conducted and substantial ^{13}C enrichment fractions reported,[20,21] but yields are presumably small.

Vibration-to-Electronic Energy Transfer

Processes similar to the ones discussed earlier occur when considering V-E transfer lasers. In such lasers, a highly vibrationally excited donor molecule transfers its energy in collisions to the electronic mode of a second, acceptor species.[22,23] The electronic configuration of the acceptor species is selected to obtain possible population inversion and subsequent laser gain on a visible or near-ultraviolet radiative transition. In order to achieve the energy transfer from $CO(v)$ to an acceptor electronic state lying above 6 eV, $CO(v > 25)$ has to be significantly populated. This constraint is not required when designing a CO gas dynamic laser since, in this case, one looks for a partial population inversion on lower vibrational levels.

At present, CO is chosen as a possible donor species, and the code is being run including the low-lying electronic energy states of CO. The details of the V-E transfer rate model used to couple the electronic states are given in the Appendix. Rates for transfer between $CO(X^1\Sigma^+)$ and both $CO(a^3\Pi)$ and $CO(A\,^1\Pi)$ have been developed and compared with data from available experiments.[13,24]

As discussed, a mixture of CO, N_2, and Ar is used to enhance the V-E transfer from $CO(X^1\Sigma^+)$ to $CO(a^3\Pi)$. An optimized nozzle is used in the calculations, estimating the shape of the effective nozzle. The length of the 15-deg half-angle expansion is 15 cm, measured from the throat. A straight channel of 85 cm length follows the expansion. Higher electronic states are not considered in this model since it has been shown that the vibrational levels of the ground state $CO(X^1\Sigma^+)$ above $v = 35$ are not excited, and therefore only $CO(a^3\Pi)$ is energetically accessible. Calculations were made for a 10%CO-10%N_2-80%Ar mixture, with stagnation conditions $T_0 = 2000$ K and $P_0 = 100$ atm. Since state-resolved data for the V-V and V-T rates for the excited electronic state $a^3\Pi$ in CO are unknown, the rate for the vth vibrational level of the excited state is presently assumed to be equal to the rate for the corresponding vth level of the CO ground state.

As described in the Appendix, the rate constant for the V-E transfer is a function of a resonance parameter C_{VE} and a pre-exponential factor $S_{VE}{}^0$. We have chosen $C_{VE} = 13.58 \times 10^{-2}$ to get the optimum of the transfer at resonance, where the energy defect between the two states is minimum. $S_{VE}{}^0$, the amplitude of the transfer, is adjusted from 10^{-11} (gas kinetic) to 10^{-14} cm^3/s. At the same time, the formation of C and CO_2 is studied (see preceding reactions); the specific rate constant for these chemical reactions is k_0 (see Appendix), which varies between 10^{-15} and 10^{-17} cm^3/s. We have neglected back reaction rate processes; for the relatively small amounts of CO reacted, however, we can realistically study the amount of CO dissociated and the influence of the chemistry on the V-E transfer.

Figure 11 shows the vibrational state populations calculated with this model, for a 15-deg half-angle expansion of 15 cm length, followed by an 85-cm straight section, to $A/A^* = 16.5$, $M = 5.5$, $P = 151.2$ Torr, and $T = 197$ K. We have chosen the V-E coupling parameter of $S_{VE}{}^0 = 5 \times 10^{-13}$ cm^3/s, and $S_{VE}{}^0/k_0 = 100$. This implies a V-E transfer rate approximately equal to the gas-kinetic collision rate and a chemical reaction approximately 100 times slower than the V-E transfer. This choice of parameters approximately reproduces previously observed coupling between the two electronic states.[14,38] Figure 11 shows the influence on the $X^1\Sigma^+$ vibrational population distribution of the V-E transfer into the $a^3\Pi$ state. The large dimple beginning near $v = 28$ is due to this

coupling; states near $v = 28$ are close to resonance for the V-E transfer from $X^1\Sigma^+$ to $a^3\Pi$. Qualitatively similar effects on V-V pumped CO($X^1\Sigma^+$, v) distributions have been measured experimentally in electric discharges by Farrenq and Rossetti.[14] The coupling becomes very weak as $S_{VE}{}^0$ is decreased below 5×10^{-14} cm^3/s.

Electronic-to-Electronic Energy Transfer

To model a CO-NO energy transfer laser, we have to study the transfer occurring between the electronic states of CO and NO (E-E transfer). A strong uv emission was reported in a previous study,[38] while CO was excited in a CO-NO mixture. The simplified model we have used in our calculations is as follows:

$$CO(X^1\Sigma^+, v>27) + NO(X^2\Pi) \rightarrow CO(X^1\Sigma^+, 0) + NO(B^2\Pi, 0)$$

$$CO(a^3\Pi, w) + NO(X^2\Pi) \rightarrow CO(X^1\Sigma^+, 0) + NO(B^2\Pi, 0)$$

The two first electronic levels of CO transfer their energy to an excited electronic state of NO. This process is shown on the potential curves in Fig. 12.

A related transfer is likely to occur from vibrationally excited levels of the electronic ground state of NO itself to NO($A^2\Sigma^+$) and to NO($B^2\Pi$).[12] The band emission from these excited NO electronic states is the well-known γ band for the system NO($A^2\Sigma^+$)-NO($X^2\Pi$) and the β band for the system NO($B^2\Pi$)-NO($X^2\Pi$). We will only consider the β band in the following calculations. It is necessary to achieve a high density of CO($X^1\Sigma^+$, $v>27$) and CO($a^3\Pi$) if one wants to excite a fair amount of NO($B^2\Pi$) in order to create a population inversion between NO($B^2\Pi$) and NO($X^2\Pi$).

The mixture is 10%CO-10%N_2-80%Ar. The stagnation conditions are $T_0 = 2000$ K and $P_0 = 100$ atm. The length of the 15-deg half-angle expansion is 15 cm; the straight channel is 85 cm long. At 80 cm from the throat, in the constant area channel, NO is injected in the mixture; the mixing is assumed to be instantaneous. Such an assumption implies that we have the maximum amount of NO in the mixture as soon as the gas reaches the mixing zone; this can be considered as the worst case since NO is a very effective quencher. The mixing zone is 20 cm long; the population of each component of the mixture is monitored at the end of the mixing zone.

The detailed mechanism and rate constants for the reactions producing NO($B^2\Pi$) are not known. The global parameter P_{EE} (see Appendix) is therefore varied from 10^{-1} to 10^{-6}. The amount of NO injected is 10% of the CO density. In order to study the possibility of a laser effect the small signal gain is calculated for the transition NO($B^2\Pi$, $v = 0$, J)→NO($X^2\Pi$, $v = 8$, $J + 1$), which corresponds to the largest Franck-Condon factor, or the most probable radiative transition. Standard expressions for Doppler-broadened gain[38] are used. The calculations show a population inversion between NO($B^2\Pi$) and NO($X^2\Pi$); the temperature achieved in the gas is 200 K. The gain (in cm^{-1}) is plotted vs the rotational quantum number J for several values of the transition probability P_{EE} in Fig. 13. The gain curves remain about the same for $P_{EE} > 10^{-3}$, showing the maximum gain that can be obtained under these conditions. It is likely that the gain is about 10^{-3} for $P_{EE} > 10^{-4}$. The wavelength of the transition is 0.323 μm in the uv range.

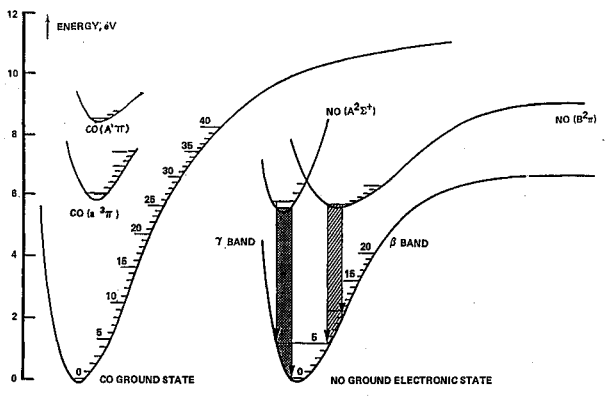

Fig. 12 CO and NO energy levels.

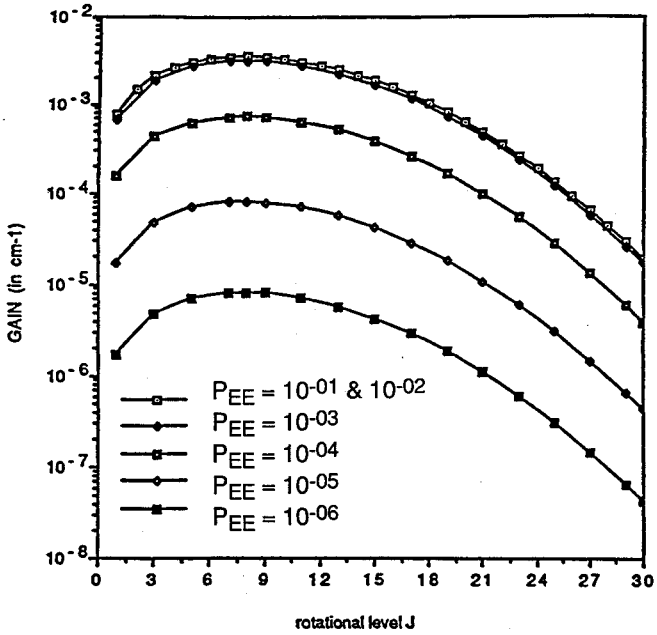

Fig. 13 CO/NO V-E/E-E transfer laser; small signal gain for NO-β at 200 K: NO($B^2\Pi$, $v = 0$, J)→NO($X^2\Pi$, $v = 8$, $J + 1$).

Conclusions

A new vibrationally nonequilibrium code has been developed, which includes vibrational-state-specific population balances, the influence of excited electronic states, and some chemical reaction channels for compressible flows of mixtures of diatomic gases. Recent theoretical and experimental rate data on vibration-to-vibration, vibration-to-electronic, and electronic-to-electronic energy transfer processes have been reviewed and used in the model. Calculations for isotopic mixtures of CO molecules, V-E, and E-E energy transfer in CO and NO are discussed in detail.

The code has been successfully applied to the design of a CO-NO energy transfer laser and can be used with other donor-acceptor pairs such as NF-IF, N_2-NO, or other systems. Uncertainties remain in the model regarding some of the mechanisms involved and some of the transfer rate constants. Although the theoretical calculations show the feasibility of such lasers, validation by experiment is necessary; new processes and unexpected mechanisms can arise due to the complexity of the electronic structures of the systems we are studying.

Appendix: Summary of Rate Expressions

We introduce $n_{i,v} = \rho_{i,v}/m_i$, the number density of the primary species i, in vibrational state v, in part/cc; $n_{j,w} = \rho_{j,w}/m_j$ the number density of the secondary species j in vibrational state w, in part/cc; $n_i = \sum_v n_{i,v}$ the total number density of species i, in part/cc; and $n_T = \sum_i n_i$ the total number density of the mixture. We have

$$\rho = \sum_{i,v} \rho_{i,v} + \sum_m \rho_m = \mu n_T$$

and

$$X_{i,v} = n_{i,v}/n_T$$

Vibration-Translation Term

The VT term of Eq. (2) is written as

$$\mathrm{VT}_i^v = \sum_j n_j \{P_{ij}^{v+1,v}[n_{i,v+1} - \exp(-\Delta E_i^v/kT)n_{i,v}] - P_{ij}^{v,v-1}[n_{i,v} - \exp(-\Delta E_i^{v-1}/kT)n_{i,v-1}]\}$$

where $P_{ij}^{v,v-1}$ is the rate constant (in cm^3/s) of the V-T transition:

$$X_i(v) + X_j \rightarrow X_i(v-1) + X_j$$

$X_i(v)$ refers to species i in vibrational state v. The rate constant can be expressed as follows[13,41]:

$$P_{ij}^{v,v-1} = P_{ij}^0(T) \cdot \frac{v}{1 - x_{ei}v} \cdot F_{ij}^{v,v-1}(\lambda_{ij}^{v,v-1})$$

F is a function given by[42]

$$F(\lambda) = \tfrac{1}{2} \cdot [3 - e^{-\frac{2}{3}\lambda}] \cdot e^{-\frac{2}{3}\lambda}$$

$$\lambda_{ij}^{v,v-1} = 2^{-3/2} \cdot \sqrt{\frac{\Theta_{ij}}{T}} \cdot \frac{|\Delta E|}{k\Theta_i}$$

where ΔE is the energy difference between the products and the reactants in the V-T transition; $\Theta_i = hc\omega_{ei}/k$ is the vibrational characteristic temperature of species i; $\Theta_{ij} = 16\pi^4\mu_{ij}c^2\omega_{ei}^2l^2/k$ is in Kelvin[25,41] where μ_{ij} is the reduced mass, c the speed of light, and $l = 0.2$ Å the range parameter. The ratio Θ_{ij}/Θ_i^2 is given in Table A1.

In the rate constant expression, $P_{ij}^0(T)$ is a coefficient that allows fitting to experimental relaxation time data. It is expressed as

$$P_{ij}^0(T) = \frac{(1 - x_{ei})kT}{\{(\tau_{ij}p) \cdot F_{ij}^{l,0} \cdot [1 - \exp(-\Theta_i/T)]\}}$$

Here, the Boltzmann constant k is in erg/K. $\tau_{ij}p$ is the vibrational relaxation time in atm.μs and is given by

$$\ln(\tau_{ij}p) = A_{ij} + B_{ij}T^{-1/3} + C_{ij}T^{-2/3}$$

A_{ij}, B_{ij}, and C_{ij} are chosen to fit the experimental data (see Table A1).

Vibration-Vibration Term

The VV term, including only the single quantum transitions, is written as

$$\mathrm{VV}_i^v = \sum_j \sum_{w=0}^{w_{\max}} \{Q_{ij_{w,w+1}}^{v+1,v}[n_{i,v+1}n_{j,w} - \exp(-\Delta E_{ij}^{v,w}/kT)n_{i,v}n_{j,w+1}] - Q_{ij_{w,w+1}}^{v,v-1}[n_{i,v}n_{j,w} - \exp(-\Delta E_{ij}^{v-1,w}/kT)n_{i,v-1}n_{j,w+1}]\}$$

$Q_{jk_{w-1,w}}^{v,v-1}$ is the rate constant (in cm^3/s) of the V-V transition:

$$X_i(v) + X_j(w-1) \rightarrow X_i(v-1) + X_j(w)$$

The rate constant is the sum of two terms, the first being the contribution of the short-range interactions, and the second the contributions of the long-range forces due to dipole-dipole interaction.[41,43-45] The rate constant has the following expression[13]:

$$Q_{ij_{w-1,w}}^{v,v-1} = Z_{ij}[S_{ij_{w-1,w}}^{v,v-1} + L_{ij_{w-1,w}}^{v,v-1}]e^{-(\Delta E/2kT)}$$

$$Z_{ij} = 4\sigma_{ij}^2\sqrt{\frac{\pi kT}{2\mu_{ij}}}$$

where Z_{ij} is the collision number and $\pi\sigma_{ij}^2$ is the cross section.

The short-range contribution is given by[41]

$$S_{ij_{w-1,w}}^{v,v-1} = S_{ij}^0 T \frac{v}{1 - x_{ei}v} \frac{w}{1 - x_{ej}w} F_{ij_{w-1,w}}^{v,v-1}(\lambda_{ij_{w,w-1}}^{v,v-1})$$

$F(\lambda)$, λ, and ΔE have the same definitions as used in the preceding discussion.

The long-range contribution is given by[44,45]

$$L_{ij_{w-1,w}}^{v,v-1} = \frac{L_{ij}^0}{T}\left(\frac{g_i^{v,v-1}}{g_i^{1,0}}\right)^2\left(\frac{g_j^{w-1,w}}{g_j^{1,0}}\right)^2 \exp\left(-\frac{\Delta E^2}{b_{ij}T}\right)$$

S_{ij}^0, L_{ij}^0, and b_{ij} are empirical parameters matched to experimental data (see Table A1). b_{ij} is in erg^2/K and

$$\left(\frac{g_i^{v,v-1}}{g_i^{1,0}}\right)^2 = \left[\frac{a_i + 1}{a_i + 3 - 2v}\right]^2\left[\frac{v(a_i + 2 - 2v)(a_i + 4 - 2v)}{a_i(a_i + 3 - v)}\right]$$

$$\left(\frac{g_j^{w-1,w}}{g_j^{1,0}}\right)^2 = \left[\frac{a_j + 1}{a_j + 3 - 2w}\right]^2\left[\frac{w(a_j + 2 - 2w)(a_j + 4 - 2w)}{a_j(a_j + 3 - w)}\right]$$

where $a_i = 1/x_{ei}$ and $a_j = 1/x_{ej}$ are the reciprocals of the anharmonicity factors.

Vibration-Electronic Term

The collision-induced V-E terms are retained only here:

$$\mathrm{VE}_i^v = n_T \sum_{j \neq i} \sum_{w=0}^{w_{\max}} S_{ij}^{v,w}\{n_{j,w} + n_{i,v}\exp[-(E_j^w - E_i^v)/kT]\}$$

where $S_{ij}^{v_i,v_j}$ is the rate constant (in cm^3/s) for the collision induced vibration-to-electronic transition:

$$X_i(v) + X \rightarrow X_j(w) + X$$

where $X_i(v)$ and $X_j(w)$ are two electronic manifolds of the same species. Their vibrational states are v and w, respectively. It is assumed that collisions can induce the transition from $X_i(v)$ to $X_j(w)$ when the energies of these molecules are very close. Such resonance occurs between $\mathrm{CO}(X^1\Sigma)$ and $\mathrm{CO}(a^3\pi)$ when the vibrational states of each electronic manifold are, respectively, $v = 27$ and $w = 0$. The rate constant is modeled with a Gaussian function of the energy defect; the width and the maximum of the Gaussian rate are empirical parameters.[38]

$$S_{ij}^{v,w} = S_{\mathrm{VE}}^0 \cdot \exp\left[-\left(\frac{\Delta E}{C_{\mathrm{VE}}\omega_e}\right)^2\right] \cdot \exp\left(-\frac{\Delta E}{2kT}\right)$$

Table 1 Parameters used in the V-T and V-V rate models

Species	A_{jk}	B_{jk}	C_{jk}	Θ_{jk}/Θ_j^2	S_{jk}^0	L_{jk}^0	b_{jk}	Reference
CO-CO	−15.23	280.5	−549.6	45.6×10^{-02}	1.64×10^{-06}	1.614	7.78×10^{-31}	13,31
CO-N_2	−7.934	147.7	0	3.295×10^{-02}	7.006×10^{-08}	1.897×10^{-02}	3.69×10^{-30}	32,36
N_2-N_2	−12.539	258.9	−390.9	18.495×10^{-02}	9.37×10^{-08}	0	1	31,33,37
CO-Ar	10.38	0	0	1.335×10^{-03}	—	—	—	13
N_2-Ar	−15.62	168.95	0	1.335×10^{-03}	—	—	—	34
CO-H_2	−4.71	62.87	0	3.4175×10^{-02}	—	—	—	35
NO-NO	3.451	−26.182	0	48.78×10^{-02}	2.428×10^{-05}	0	1	12
NO-CO	−0.658	13.274	0	47.19×10^{-02}	3.37×10^{-06}	0	1	38-40
NO-N_2	6.4338	0	0	3.525×10^{-02}	1.55×10^{-08}	0	1	38-40
NO-Ar	10.38	0	0	1.335×10^{-03}	—	—	—	This work

The vibrational spectroscopic constant ω_e is taken to be the larger of the constants for the two electronic states involved. The adjustable parameters are S^0_{VE} and C_{VE}. In the case of $CO(X^1\Sigma) \rightarrow CO(A^1\Pi)$ and $NO(X^2\Pi) \rightarrow NO(B^2\Pi)$ transfers, values of these parameters were obtained by fitting kinetic rate models to V-V up-pumping experiments in optical cells.[12,13,24] For the case of $CO(X^1\Sigma) \rightarrow CO(a^3\Pi)$, there are no comparable data, although indication of the coupling has been seen in the experiments of Farrenq and Rossetti.[14] The range of validity of the preceding resonance model remains to be determined in detailed state-resolved experiments. In Table A2, the value of these parameters are indicated.

Electronic-Electronic Term

The E-E transfer terms are written as

$$EE_{CO(a^3\Pi,w)} = -k_{EE} n_{CO(a^3\Pi,w)} n_{NO(X^2\Pi)}$$

$$EE_{CO(X^1\Sigma^+,0)} = k_{EE}[n_{CO(a^3\Pi,w)} + n_{CO(X^1\Sigma^+,v\geq 28)}] n_{NO(X^2\Pi)}$$

$$EE_{CO(X^1\Sigma^+,v\geq 28)} = -k_{EE} n_{CO(X^1\Sigma^+,v\geq 28)} n_{NO(X^2\Pi)}$$

$$EE_{NO(B^2\Pi,0)} = -EE_{NO(X^2\Pi)} = EE_{CO(X^1\Sigma^+,0)}$$

The rate constant for the electronic-electronic processes k_{EE} is expressed as follows[38]:

$$k_{EE} = P_{EE} \cdot Z_{CO-NO}$$

P_{EE} is the probability of transfer and Z_{CO-NO} is the collision number. This number represents the number of collisions between CO and NO during 1 s in 1 cm^3. P_{EE} is then the percentage of collisions needed for the reaction to proceed. P_{EE} is treated as a parameter in the calculations, as discussed in the text. One can calculate Z_{CO-NO} (in cm^3/s)

$$Z_{CO-NO} = 3.10^{-10}\sqrt{\frac{T}{300}}$$

Spontaneous Radiative Decay Term

The spontaneous radiative transfer term is written as

$$SRD_i^v = \sum_u [A_i^{v+u,v} n_{i,v+u} - A_i^{v,v-u} n_{i,v}]$$

The rates for the spontaneous radiative decay A have been calculated with the Einstein coefficients for radiative transitions between vibrational levels within the same electronic state and with the Franck-Condon factors for the radiative transitions between vibrational levels of different electronic states.[26]

Chemical Reactions Rate Model

We consider the reaction of CO during the expansion in the nozzle. The reactants can be CO isotopes in the two first electronic states, $CO(X^1\Sigma)$ or $CO(a^3\Pi)$. The reaction is the following:

$$CO(v) + CO(w) \rightarrow CO_2 + C$$

The activation energy of this reaction is $E_a = 6$ eV.

The chemical terms are written as

$$CHM_C = CHM_{CO_2} = \sum_{v,w}{}' k_w^v n_{CO,v} n_{CO,w}$$

$$CHM_{CO,v} = CHM_{CO,w} = -k_w^v n_{CO,v} n_{CO,w}$$

The rate model[27] is the following:

$$k_w^v = k_0\sqrt{\frac{T}{300}}\left(1 - \frac{E_a}{E_{CO,v} + E_{CO,w}}\right)^2$$

Table 2 Parameters used in the V-E rate model

Transitions	C_{VE}	S^0_{VE}	Reference
$CO(X^1\Sigma^+)$-$CO(a^3\Pi)$	13.58×10^{-02}	5.0×10^{-13}	This work
$CO(X^1\Sigma^+)$-$CO(A^1\Pi)$	5.49×10^{-02}	9.94×10^{-13}	13
$NO(X^2\Pi)$-$NO(B^2\Pi)$	8.0×10^{-02}	3.938×10^{-10}	12

where $E_{CO,v}$ is the energy of $CO(v)$ and k_0 is an adjustable parameter. $k_0 = 0$ when $E_{CO,v} + E_{CO,w} \leq E_a$. The value of k_0 is presently being inferred from experiments.[28,29] In the present calculation, the value $k_0 = 5 \times 10^{-15}$ cm^3/s is used.

Spectroscopic Constants[30]

All of the spectroscopic constants are expressed in cm^{-1}. The spectroscopic constants have been determined by mass scaling of the constants of ^{12}CO for ^{13}CO.

Parameters Used in the Rate Expressions

The parameters used in the expression of the V-T and V-V rates are indicated in Table A1. The rate constants involving ^{13}CO are taken to be the same as for ^{12}CO. For studying the effect of H_2 in the mixture, the V-T rate N_2-H_2 is assumed to be the same as for H_2-CO; H_2 is considered as a diluent and is not vibrationally active. We take n-H_2 in the model (the normal mixture ratio of o-H_2 and p-H_2).

Acknowledgments

This research was supported by Pacific Applied Research, under prime contract from the U.S. Strategic Defense Initiative Office/IST, and administered by Los Alamos National Laboratory, and by the Aero Propulsion and Power Laboratory, Aeronautical Systems Division, Wright Research and Development Center.

References

[1]Moss, J. N., Cuda, V., and Simmonds, A. L., "Nonequilibrium Effects for Hypersonic Transitional Flows," AIAA Paper 87-0404, Jan. 1987.

[2]Bussing, T. R. A., and Eberhardt, S., "Chemistry Associated with Hypersonic Vehicles," AIAA Paper 87-1292, June 1987.

[3]Sharma, S. P., and Gillespie, W., "Nonequilibrium and Equilibrium Shock Front Radiation Measurements," *Journal of Thermophysics and Heat Transfer,* Vol. 5, No. 3, 1991, pp. 257–265.

[4]Rusanov, V. D., Fridman, A. A., and Sholin, G. V., "The Physics of a Chemically Active Plasma with Nonequilibrium Vibrational Excitation of Molecules," *Soviet Physics Uspekhi,* Vol. 24, No. 6, 1981, pp. 447–474.

[5]McDaniel, E. W., and Nighan, W. L., "Applied Atomic Collision Physics," *Gas Lasers,* Vol. 3, Academic, New York, 1982.

[6]Treanor, C. E., Rich, J. W., and Rehm, R. G., "Vibrational Relaxation of Anharmonic Oscillators with Exchange-Dominated Collisions," *Journal of Chemical Physics,* Vol. 48, No. 4, 1968, pp. 1798–1807.

[7]Capitelli, M., (ed.), *Nonequilibrium Vibrational Kinetics,* Springer-Verlag, Berlin, 1986.

[8]Anderson, J. D., Jr., *Gasdynamic Lasers: An Introduction,* Academic, New York, 1976.

[9]McKenzie, R. L., "Diatomic Gasdynamic Lasers," *Physics of Fluids,* Vol. 15, No. 12, 1972, pp. 2163–2173.

[10]Cherkasov, E. M., and Chesnokov, V. I., "Numerical Optimization of Parameters of CO Gasdynamic Lasers," *Soviet Journal of Quantum Electronics,* Vol. 18, No. 3, 1988, pp. 301–306.

[11]Gorse, C., Cacciatore, M., and Capitelli, M., "Kinetic Processes in Non-equilibrium Carbon Monoxide Discharges. I. Vibrational Kinetics and Dissociation Rates," *Chemical Physics,* Vol. 85, No. 2, 1984, pp. 165–176.

[12]Dünnwald, H., Siegel, E., Urban, W., Rich, J. W., Homicz, G. F., and Williams, M. J., "Anharmonic Vibration-Vibration Pumping in Nitric Oxide by Resonant IR-laser Irradiation," *Chemical Physics,* Vol. 94, No. 1, 1985, pp. 195–213.

[13]Deleon, R. L., and Rich, J. W., "Vibrational Energy Exchange Rates in Carbon Monoxide," *Chemical Physics,* Vol. 107, No. 2, 1986, pp. 283–292.

[14]Farrenq, R., and Rossetti, C., "Vibrational Distribution Function in a Mixture of Excited Isotopic CO Molecules," *Chemical*

Physics, Vol. 92, No. 2, 1985, pp. 401–416.

[15]Hindmarsh, A. C., "LSODE and LSODI, Two Initial Value Ordinary Differential Equation Solvers," *ACM SIGNUM Newsletter,* Vol. 15, 1980, pp. 10–11.

[16]Oran, E. S., and Boris, J. P., *Numerical Simulation of Reactive Flow,* Elsevier, New York, 1987.

[17]Andronov, G. A., Armer, A. G., Belavin, V. A., Dymshits, B. M., Koretskii, Y. P., and Sharkov, V. F., "Gasdynamic Laser Using a CO-Ar Mixture," *Soviet Journal of Quantum Electronics,* Vol. 7, No. 8, 1977, pp. 1023–1024.

[18]Rich, J. W., Bergman, R. C., and Lordi, J. A., "Electronically Excited, Supersonic Flow Carbon Monoxide Laser," *AIAA Journal,* Vol. 13, No. 1, 1975, pp. 95–101.

[19]Dunn, O., Harteck, P., and Dondes, S., "Isotopic Enrichment of Carbon-13 and Oxygen-18 in the Ultraviolet Photolysis of Carbon Monoxide," *Journal of Physical Chemistry,* Vol. 77, No. 7, 1973, pp. 878–883.

[20]Akulintsev, V. M., Gorshunov, N. M., Neshchimenko, Y. P., Ostroglazov, A. A., Perov, A. A., Samsonov, G. A., Stepanov, A. A., and Shikanov, A. A., "Separation of Carbon Isotopes in an Expanding Supersonic Flow," *Soviet Technical Physics Letters,* Vol. 8, No. 3, 1982, pp. 119–120.

[21]Akulintsev, V. M., Gorshunov, N. M., Neshchimenko, Y. P., and Shikanov, A. A., "Isotope Separation in Nonequilibrium Chemically Reacting Supersonic Flows," *Soviet Physics: Technical Physics,* Vol. 29, No. 8, 1984, pp. 918–920.

[22]Kochelap, V. A., Izmailov, I. A., and Mel'nikov, L. Y., "The Possibility of Population Inversion and Light Gain Due to Electronic Energy Transfer from $N_2(A^3\Sigma_u^+)$," *Chemical Physics Letters,* Vol. 157, Nos. 1–2, 1989, pp. 67–72.

[23]Basov, N. G., Gavrikov, V. F., Pozdneev, S. A., and Shcheglov, V. A., "Possible Expansion of the Spectral Emission Range of Electronic-Transition Chemical Lasers," *Soviet Journal of Quantum Electronics,* Vol. 17, No. 9, 1987, pp. 1139–1153.

[24]Urban, W., Lin, J.-X., Subramaniam, V. V., Havenith M., and Rich, J. W., "Treanor Pumping of CO Initiated by CO Laser Excitation," *Chemical Physics,* Vol. 130, 1989, pp. 389–399.

[25]Yardley, J. T., *Introduction to Molecular Energy Transfer,* Academic, New York, 1980.

[26]Krupenie, P. H., "The Band Spectrum of Carbon Monoxide," *National Standard Reference Data Series,* NSRDS-NBS 5, Washington, DC, 1966.

[27]Rusanov, V. D., Fridman, A. A., and Sholin, G. V., "The Effect of Non-Boltzmann Population of Vibrationally Excited States on the Carbon Reduction in a Nonequilibrium Plasma," *Soviet Physics Doklady,* Vol. 22, No. 12, 1977, pp. 757–759.

[28]Gorse, C., Billing, G. D., Cacciatore, M., Capitelli, M., and De Benedictis, S., "Non-equilibrium Vibrational Kinetics of CO Pumped by Vibrationally Excited Nitrogen Molecules: General Theoretical Considerations," *Chemical Physics,* Vol. 111, No. 3, 1987, pp. 351–360.

[29]De Benedictis, S., Cramarossa F., and Achasov, O. V., "Homogeneous and Heterogeneous CO Chemical Kinetics in Liquid-nitrogen Cooled 5% CO-He Discharges," *Chemical Physics,* Vol. 124, No. 1, 1988, pp. 91–101.

[30]Huber, K. P., and Herzberg, G., "Constants of Diatomic Molecules," *Molecular Spectra and Molecular Structure,* Vol. 4, Van Nostrand Reinhold, New York, 1978.

[31]Billing, G. D., "Vibration-Vibration and Vibration-Translation Energy Transfer, Including Multiquantum Transitions in Atom-Diatom and Diatom-Diatom Collisions," *Nonequilibrium Vibrational Kinetics,* Springer-Verlag, Berlin Heidelberg, 1986.

[32]Cacciatore, M., Capitelli, M., and Billing, G. D., "Theoretical Semiclassical Investigation of the Vibrational Relaxation of CO Colliding with N_2," *Chemical Physics,* Vol. 89, No. 1, 1984, pp. 17–31.

[33]Millikan, R. C., and White, D. R., "Systematics of Vibrational Relaxation," *Journal of Chemical Physics,* Vol. 39, No. 12, 1963, pp. 3209–3213.

[34]McLaughin, D. F., and Christiansen, W. H., "Isotope Separation and Yield Calculation for Vibrationally Enhanced Oxidation of Nitrogen," *Journal of Chemical Physics,* Vol. 84, No. 5, 1986, pp. 2643–2648.

[35]Poulsen, L. L., and Billing, G. D., "Vibrational Deactivation of CO($v = 1$) by p-H_2. The Importance of the Higher-order Multipole Moments," *Chemical Physics,* Vol. 89, No. 2, 1984, pp. 219–222.

[36]Billing, G. D., "Vibration/Vibration Energy Transfer in CO Colliding N_2," *Chemical Physics,* Vol. 50, No. 2, 1980, pp. 165–173.

[37]Akishev, Y., Dem'yanov, A. V., Kochetov, I. V., Napartovich, A. P., Pashkin, S. V., Ponomarenko, V. V., Pevgov, V. G., and Podobedov, V. B., "Determination of Vibrational Rate Constants in N_2 by Gas Heating," *Teplofizika Vysokikh Temperature,* Vol. 20, No. 5, 1982, pp. 818–827.

[38]Rich, J. W., Bergman, R. C., and Williams, M. J., "Vibration to Electronic Energy Transfer Laser," Calspan Rept. 6678-A-2, Buffalo, NY, April 1984.

[39]Stephenson, J. C., "Vibrational Relaxation of NO $X^2\Pi(v = 1)$ in the Temperature Range 100–300°K," *Journal of Chemical Physics,* Vol. 60, June 1974, pp. 4289–4294.

[40]Breshears, W. D., and Bird, P. F., "Vibrational Relaxation of Nitric Oxide at 500–1,900 K," *Nature,* Vol. 224, Oct. 1969, pp. 268–268.

[41]Schwartz, R. N., and Herzfeld, K. F., "Vibrational Relaxation Times in Gases (Three-Dimensional Treatment)," *Journal of Chemical Physics,* Vol. 22, No. 5, 1954, pp. 767–773.

[42]Keck, J., and Carrier, G., "Diffusion Theory of Nonequilibrium Dissociation and Recombination," *Journal of Chemical Physics,* Vol. 43, No. 7, 1965, pp. 2284–2298.

[43]Jeffers, W. Q., and Kelley, J. D., "Calculations of V-V Transfer Probabilities in CO-CO Collisions," *Journal of Chemical Physics,* Vol. 55, No. 9, 1971, pp. 4433–4437.

[44]Sharma, R. D., and Brau, C. A., "Energy Transfer in Near-Resonant Molecular Collisions Due to Long-range Forces with the Application to Transfer of Vibrational Energy from ν_3 Mode of CO_2 to N_2," *Journal of Chemical Physics,* Vol. 50, No. 2, 1969, pp. 924–930.

[45]Rich, J. W., Lordi, J. A., Gibson, R. A., and Kang, S. W., "Supersonic Electrically Excited Laser Development," Calspan Rept. WG-5164-A-3, Buffalo, NY, June 1974.

[46]Likalter, A. A., and Naidis, G. V., "On the Vibrational Relaxation of Diatomic Molecules at Intermediate Excitation," *Chemical Physics Letters,* Vol. 59, No. 2, 1978, pp. 365–368.